2nd International Symposium on Magnetic Beaing
July 12-14, 1990, Tokyo, Japan

EXTREME PRECISION MAGNETIC BEARINGS FOR LINEAR AND ROTARY APPLICATIONS

David B. Eisenhaure*, James R. Downer*, Richard L. Hockney*, Bruce G. Johnson*,
Vijay Gondhalekar*, Michael Gerver*, Kathleen Misovec*, Monique Gaffney*, Alex Slocum**
*SatCon Technology Corporation, 12 Emily Street, Cambridge, MA 02176 USA
**Massachusetts Institute of Technology, Civil Engineering, Cambridge, MA 02139

Abstract

SatCon Technology Corporation is developing magnetic bearings and suspensions for a number of linear and rotary applications which require positioning accuracies considerably higher than those obtainable with passive mechanical bearings. These applications, which include instrument bearings, magneto-optical data storage, tunneling microscope slides, and machine tool spindles require positioning accuracies as high as 10^{-6} mm over a broad frequency range in the presence of environmental disturbances. Obtaining these levels of precision in active magnetic bearings requires new developments in sensor, actuator, and control subsystems. Substantial technology advances have occurred during the last decade that have an appreciable impact on the performance and feasibility of magnetic bearings for precise positioning applications. These advances in technology include improvements in sensors, magnetic materials, improved semiconductor power electronics, improved digital electronics, and better control system technology. This paper compares and contrasts the design approaches for major magnetic bearing subsystems in these applications that SatCon currently has under development. The achievable resolution is shown to be determined by position measurement accuracy, suspension gain, suspension bandwidth, internal component noise, and external disturbance force levels. Expected external disturbance force levels from ground motion, air currents, and acoustic effects are projected. Given the expected disturbance force levels, measurement accuracy, and required controller performance, magnetic suspensions and bearings can be developed which will provide positioning accuracies better than the 10^{-6} mm (ten Angstroms) required.

1. Introduction

In the sensor area precision positioning requires sensors with high precision, wide bandwidth, and low noise. Optical interferometric sensors currently provide accuracies approaching the 10^{-6} mm requirement and are expected to substantially exceed this figure in the near future. Precision inductive and capacitive sensors although not as precise as optical sensors, provide simple low-cost measurements which have sufficient precision for less demanding applications.

The need in the actuator area is for high specific-performance designs having wide bandwidth and good plant characteristics. In its various designs, SatCon is employing biased/-unbiased electromagnet, electrodynamic, and superconducting actuators. Superconducting actuators have the highest performance potential, widest bandwidth, and have good plant characteristics with minimal high frequency dynamics. Superconductors allow the construction of magnetic devices 10 or more times lighter than conventional magnetics, and the recent development of high temperature superconducting material holds much promise for the future. Advances have taken place in magnetic steels, amorphides, and permanent magnets, all of which contribute to improved electromagnet and electrodynamic actuators. In the magnetic steel area, materials such as vanadium permendur allow operating flux densities exceeding two Tesla. In the area of amorphides, materials such as Met-Glas allow high-frequency, low-loss operation. Permanent magnet materials such as samarium-cobalt and neodymium-iron have energy products approaching 40 MGOe and allow lightweight, high-efficiency magnetic designs.

In the control-system area, techniques to efficiently handle multi-input/multi-output, non-linear systems and time-varying systems with wide-bandwidth environmental disturbances are needed. SatCon's approaches for handling multi-input/output systems include linear-quadratic-Gaussian-control, loop-transfer-recovery, disturbance accommodating control, and model-reference-control techniques. In systems where non-linear effects are significant we have employed sliding-mode or variable structure, time-delay, and non-linear-quadratic-Gaussian-control methods. Adaptive control techniques such as self-tuning regulation are readily adapted to time-varying systems and those with uncertain parameters. SatCon has made particular advances in the application of sliding mode and disturbance accommodating control to precision magnetic bearings.

2. MIT/SatCon Magnetically Suspended Linear Slide

Current designs of precision machines such as wafer steppers and diamond turning machines are generally performance limited by mechanical contact between moving parts, misalignment between actuators and bearings, stability of air bearings, and/or attainable temperature control. An example of a system which uses magnetic suspensions to obtain extreme precision by eliminating or reducing many of these problems is the Atomic Resolution Measuring Machine being developed by SatCon and MIT. This system is depicted in Figure 1. The baseline slide has approximate envelope dimensions of 12 inches by 6 inches by 2 inches. This baseline slide would have a weight in Earth's gravity of ten pounds. In this paper the baseline ARMM will be used as a conceptual model to examine the issues associated with extreme precision magnetic bearing and suspension design. The analysis assumes that the slide dynamics are beyond the bandwidth of the magnetic bearing and will not be a factor in the suspension's performance.

The baseline magnetic suspension block diagram is shown in Figure 2. The principle of operation of a magnetic suspension system is quite simple: the position of the suspended slide is measured and the control system regulates the current to an electromagnet by a gain the slide at the desired location. A simple control system might be characterized by a gain (stiffness) which relates errors in position to applied magnetic force and a bandwidth which

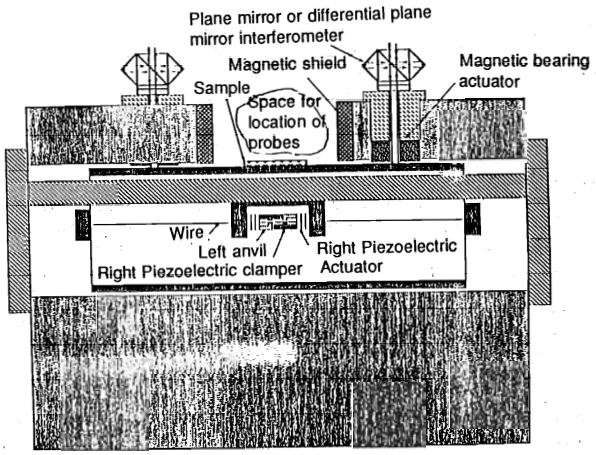

Figure 1. Cutaway side view of Atomic Resolution Measuring Machine (ARMM)

indicates the frequency range over which the magnetic force may be applied. In addition to gain and bandwidth, the control system would require electronic compensation for stable operation. Magnetic suspensions generally have unstable plant characteristics which lead to a minimum required system bandwidth for stability of about 10 Hz for many suspensions. Maximum achievable bandwidths could range from 100 Hz for a simple attractive system to 40 KHz or higher for systems implemented with ferrite or voice coil actuators. As with all position control servos, accuracy is determined by position measurement accuracy, controller gain, controller bandwidth, internal component noise. and external disturbance forces acting on the suspended slide. The remainder of this paper examines in detail the control system options together with the sensor and actuator characteristics required to achieve extremely high positioning precision.

3. Control System Developments

Satcon's efforts in the control area have been directed at developing both hardware and control algorithm solutions to the problem of precision motion control with electromagnetic actuators in the presence of environmental and internal disturbances. Over the past two years, significant advances have been made in applying nonlinear control algorithms to the nonlinear attraction force electromagnetic suspensions and using disturbance accommodating control theory to reduce vibrations in magnetic bearing systems. The use of these advanced control algorithms has been made possible by advances in digital signal processing hardware.

In many of our rotor systems, magnetic bearings have been chosen because of their capability to reduce vibration and noise. One advantage of magnetic bearings in reducing vibration, of course, is their non-contacting nature. Since they are actively controlled, the dynamics of the bearing can be tailored to both reduce transmitted vibrations and to attenuate vibrations of the machinery base. Like all actively controlled systems, however, actively controlled magnetic bearings can amplify sensor and electrical noise. As discussed below, these sensor noise effects can become the dominant noise source in precision applications where the environment is relatively quiet.

One of the most promising areas for increased performance by actively controlled magnetic bearings is reducing the synchronous vibrations produced by rotor mass unbalance. In magnetic bearing systems, these mass unbalance effects are seen as additive output disturbances in the feedback loop. The mass unbalance disturbance are seen primarily as a sinusoidal error at the synchronous frequency. At SatCon, we are developing controllers using Disturbance Accommodating Control (DAC) theory to reject these mass unbalance effects and allow the rotor to spin about its principal axis at all rotational speeds.

Disturbance accommodating control theory applies to systems with disturbances that have a waveform structure. Consequently, reducing the synchronous vibrations of rotating systems is a good application for DAC theory because the disturbances possess a waveform structure. As

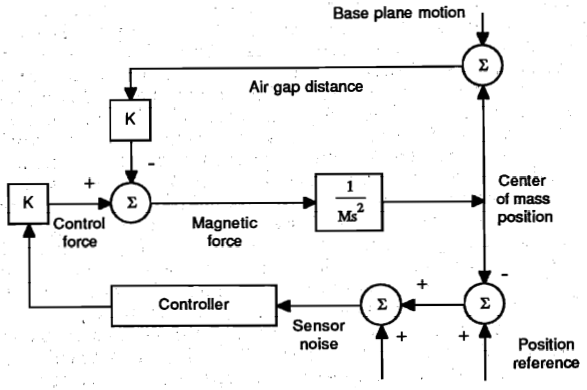

Figure 2. Basic Magnetic Suspension Block Diagram

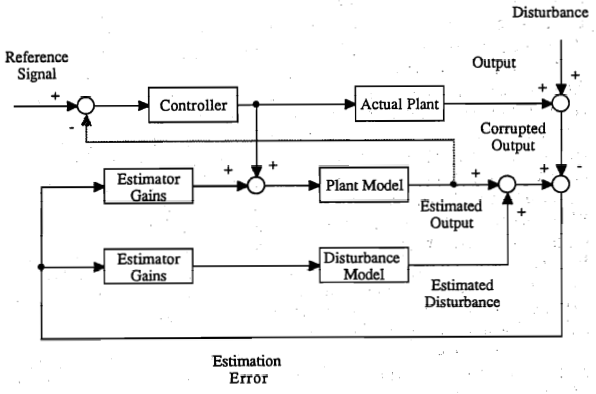

Figure 3. Disturbance Accommodating Control Block Diagram

can be seen in Figure 3, the DAC controller uses both a plant and disturbance model in the estimator, allowing accurate estimates of both the plant states and the disturbance. DAC theory is being used at SatCon to develop control/estimation schemes that enable the rotor to spin about its center of mass, in the presence of either synchronous magnetic unbalance disturbances or the measurement error (mass unbalance) disturbances. Our simulation results show excellent rejection of either disturbance at the synchronous frequency, thereby reducing the production of vibrations by the rotating system. We are currently constructing a 80 kg , 3600 rpm magnetically suspended rotor testbed that will use the DAC controller.

In the last two years, we have been investigating the use of various nonlinear control algorithms with the inherently nonlinear actuators that conventional attraction force electromagnetic bearings represent. These have included sliding mode or variable structure, time-delay, and nonlinear quadratic Gaussian methods. We have found that these nonlinear controllers have significant performance advantages over more conventional controllers at the cost of increased design, analysis, and implementation complexity.

We have implemented a sliding mode controller on a three-degree-of-freedom precision pointing and tracking testbed. This testbed uses attraction force electromagnet to slew a isolated mass through a desired trajectory. The control algorithm must provide the proper slew forces in the presence of experimentally controlled vibrations applied to the stators of the actuators. The goal is to minimize the tracking error in the presence of these vibrations.

As shown in Figure 4, the sliding mode controller uses measured gap information to invert the nonlinear force/current/gap relation of the actuators. Additional feedback loops guarantee stability in the presence of bounded disturbances and modelling error. This rather complicated block diagram illustrates the structure of the sliding mode controller. An actuator produces a control force which changes the inertial position of the tracking body (plant). Vibration disturbances can change the magnetic gap, which also changes the control force and thus there is a path between vibration disturbance and inertial position. The sliding mode controller has the potential to achiever better performance than the linear controller because it has a structure that directly compensates for this vibration path. More specifically, an estimation scheme produces estimated gaps and the controller uses a nonlinear model of the plant to counteract the effect of the vibration disturbance. The controller also uses estimated position and velocities to calculate control currents that are similar to a PD type of controller but are calculated to insure stability in the presence of the effect of bounded modelling uncertainty and disturbances. our research has shown that in order to achieve performance advantages over linear controllers, the sliding mode controller depends heavily on a good inertial measurement and estimation as well as highly accurate plant models.

Figure 5. shows the performance of this controller compared to more conventional linear controllers. We were interested in assessing the performance of the nonlinear sliding mode control approach to: a linear phase lead controller and a

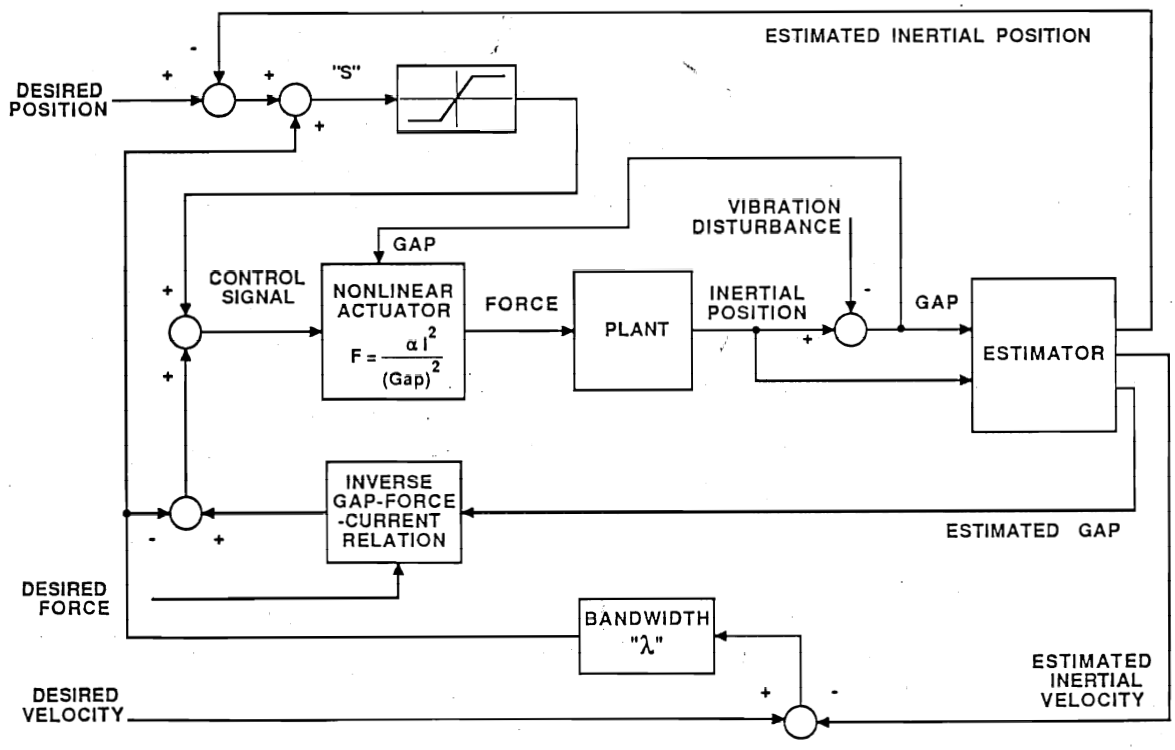

Figure 4. Sliding Mode Control Block Diagram

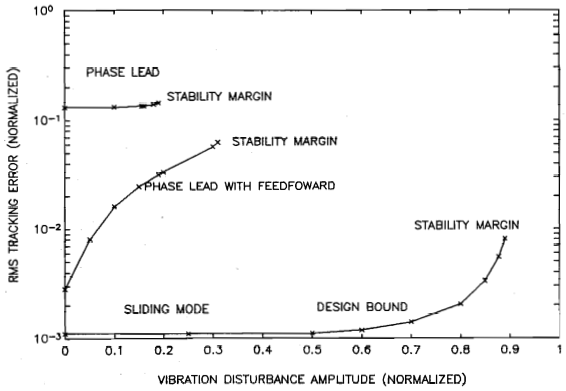

Figure 5. Sliding Mode Control Tracking Air vs Vibration Amplitude

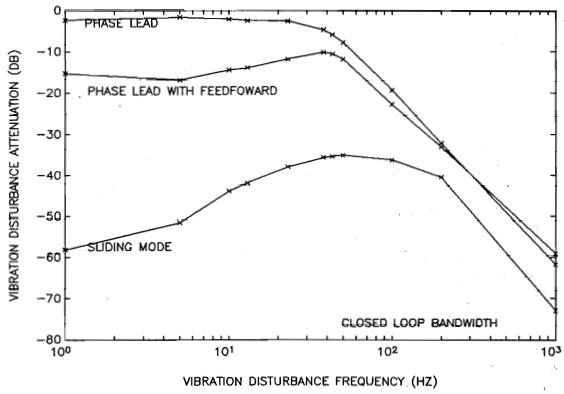

Figure 6. Sliding Mode Control Vibration Isolation vs Frequency

phase lead with a feedforward term. This plot is based on simulations of a tracking maneuver in the presence of a vibration disturbance for these three controllers. The performance measure of RMS tracking error is plotted, vs the vibration disturbance amplitude. The sliding mode controller achieves better tracking performance by at least an order of magnitude. The sliding mode controller also has higher stability margins than the more conventional control approaches. The stability margin is reached when the tracking error is high enough to cause the magnetic gaps to go to zero. The sliding mode controller in these simulations is designed for the maximum disturbance amplitude shown in the figure. An even higher stability margin could be obtained by increasing the design bound at the expense of higher tracking error.

Another performance measure to use to assess the potential of sliding mode control in comparison to more conventional linearized control approaches is vibration disturbance attenuation shown in figure 6.. This is a measure of how much disturbance energy is being transmitted to the tracking body. This plot shows vibration disturbance attenuation vs vibration disturbance frequency. The sliding mode controller achieves better disturbance attenuation that the phase lead or the phase lead with feedforward approaches. We were particularly interested in performance near the closed loop bandwidth. Better linear controllers can be designed for disturbances below the bandwidth, but all linear controllers have a limited attenuation capability when the disturbances are near the system bandwidth. This is due to fundamental physical considerations and the structure of the controller. For these simulations, analysis indicated this limiting performance value to be around -9 dB for the linearized approaches. The plot shows that this limitation is accurate for the linear controller and that the sliding mode controller, because of its different structure, is not limited to this performance value. It is achieving about -40 dB at disturbance frequencies near the closed loop bandwidth.

As mentioned earlier, the use of these advanced control algorithm is predicated on high performance, low cost digital signal processors. The advances made in digital signal processors and associated software development tools have gone a long way towards reducing the cost in real terms of implementing complex signal conditioning and digital control algorithms. When applied to the control of precision magnetic bearings where fairly complex algorithms are implemented, the number crunching capability per dollar delivered by the DSPs is very rewarding.

However there is an inherent limitation, at least currently at the low cost end, of the signal resolution delivered by interface electronics, principally the digital to analogue convertors. The expanding digital audio market has promoted low cost 16 bit convertors which give a resolution approaching 15 ppm. Moderate cost 20-22 bit convertors may be expected in the near future which will be adequate to deliver a 1 ppm signal resolution at the signal input end of the digital signal processor.

A very important advantage offered by digital signal processors is the ability to easily implementing error correction logic to the incoming measurement data stream from the A/D convertors. This of course relieves to a certain extent the burden and cost of designing linear and environmentally insensitive sensors. The extra computational effort for error correction itself is usually small, however the quality of correction depends on the error modelling and extra information, such as temperature, made available to the model. The influence on the cost of the "total" sensor system is more from the hardware associated with obtaining this extra information.

Floating point arithmetic DSPs and the available development tools have gone a long way towards elevating the programmers task by eliminating scaling as with integer math DSPs. However quantization noise generated by the finite precision imposed by the finite word length architecture can become a serious impediment when implementing signal processing or control algorithms requiring a large number of mathematical operations on the raw data. Specialized large word length machines which retain full precision of any arithmetic operation by using integer math and dynamically expanding the word length may become a necessity for an extreme precise implementation of control algorithms. However this type of machines are not likely to be available at the low cost end.

SatCon's implementation of the sliding mode control algorithm mentioned above is based on a integer math DSP utilizing 12 bit signal inputs an a 32 bit internal number precision. Although routines were developed for higher precision math these were not used in view of the low precision available on the raw data and the inherent execution time penalties. Currently the control of a superconducting magnet large angle magnetic suspension is being implemented on a floating point DSP. The application is numerically intensive as a result of the large number of geometrical transforms involved in the signal processing stage and is expected to fully utilize the floating point capability of the TMS320C30 selected for the implementation.

4. Position Measurement

The fundamental requirements for sensors which measure the position of the suspended object are that they be non-contacting, and capable of sensing the total dynamic range of motion, typically twice the magnetic air-gap or about 1 mm. The basic sensor types applicable to this task are capacitive, inductive, eddy-current and photo-electric where the latter category includes both the diffuse-reflective type and interferometers. Ultra-precision positioning requires levels of stability and resolution that eliminate the diffuse-reflective in all applications and inductive sensors in many applications. The sensitivity of the diffuse-reflective sensor to both surface finish and contaminants make its use inappropriate. In the case of the inductive sensor, changes in the incremental permeability of the target material due to the variations in ambient magnetic field make nanometer resolution impossible for sensors co-located with the actuators. Interferometers capable of 1 mm dynamic range routinely provide nanometer resolution and stability, but are physically large, require a mirrored surface, and cost approximately $10,000 per channel. Thus, achieving nanometer resolution with either the eddy-current or capacitive sensors would greatly reduce both system cost and complexity. In addition, since both these techniques effectively average information over a relatively large surface area, microscopic surface-finish features are unimportant.

Capacitive position sensors measure the capacitance of the air-gap between the sensor electrode and the target. Eddy-current sensors measure the loss in the target material induced by the time-varying magnetic field created by the probe.

Both sensors perform best with a non-magnetic metallic target, and are extremely linear over a specified range. Both also employ measurement electronics which measure the impedance of the sensor: $x_c = j\ _oC$ for the capacitive and loss resistance for the eddy-current. This then involves the measurement of both voltage and current for both types. First order calculations indicate the combined resolution achievable with these two measurements is one part in 10^5, indicating 10 nm is a reasonable goal.

The stability of measurements made with the capacitive and eddy-current sensors is predominantly influenced by the temperature sensitivity of the physical property used in the measurement process. Both the dielectric constant of air and the resistivity of aluminum have a temperature coefficient of about 0.5%/°C, which indicates a required temperature stability on the order of 10^{-3}°C. This requirement can be reduced significantly by employing two identical sensors in a bridge configuration, where variations in thermal gradients will become the predominant error source. Since temperature gradient control is necessary for many aspects of these ultra-precision applications, such techniques as virtual-zero-power suspension or constant power actuators will be used in any event as discussed previously.

4.1 Theoretical Limits on Sensor Precision

We have examined the limitations on the precision of capacitive, inductive, and eddy current sensors imposed by the following fundamental sources of noise: 1) thermal noise, sometimes called Johnson noise, whose magnitude is given by the Nyquist theorem; 2) Barkausen events in ferromagnetic materials, which cause the B-H curve, and hence the permeability, to be slightly different, in a random way, on each cycle, introducing noise in inductive sensors, 3) the Heisenberg uncertainty principle of quantum mechanics, which limits the precision by which energy (and hence potential) can be measured if the measurement is done in a finite time; and 4) the finite charge of an electron, which limits the precision to which current can be measured in a finite time. The limitations on precision imposed by these sources of noise have been compared with the limitations of 15 ppm or 1 ppm imposed by the digital to analog converters, in order to determine when these other sources of noise might impose more severe limitations than the digital electronics, and in order to see at what point one would run into these limitations if the resolution of the electronics is further improved in the future.

Any type of sensor has a characteristic length d representing the range over which it has a linear response. In the case of the inductive and eddy current sensors, d is the largest dimension of the coil, whether length or diameter, and in the case of capacitive sensors d is the gap distance. Within the linear range, the uncertainty in position Δx is related to the uncertainty in voltage ΔV for inductive sensors by

$$\Delta x = d\ \Delta V/I_c L\omega \qquad (1)$$

where I_c is the current in the coil, L is the inductance of the coil, and ω is the frequency with which the probe is being excited. For eddy current sensors

$$\Delta x = d\ \Delta V/I_r R_{eddy} \qquad (2)$$

where

$$R_{eddy} = L\omega(1 + \rho_r/\mu_r\omega d^2)^{-1} \qquad (3)$$

is the part of the resistive impedance of the coil due to the current induced in the rotor. For capacitive sensors,

$$\Delta x = d\ \Delta V\ \omega C/I_c \qquad (4)$$

where C is the capacitance.

The contribution to ΔV from the digital electronics is

$$\Delta V_{digit} = 1.5 \times 10^{-5}V \text{ or } 10^{-6}V \qquad (5)$$

where $V = I_c(R_{wire} + i/\omega C)$ for capacitive sensors (with R_{wire} being the resistance of the lead wires attached to the sensor), $V = I_c(R_{coil} + R_{eddy} + iL\omega)$ for eddy current sensors (with R_{coil} being the coil resistance), and $V = I_c(R_{coil} + R_{eddy} + R_{hys} + iL\omega)$ for inductive coils. Here R_{hys} is the part of the resistive impedance of the coil due to hysteresis in the rotor

$$R_{hys} \simeq (I_c \nu \omega \mu_0^3/3\pi\mu_r^3)(1 + \mu_r \omega d^2/\rho_r)^{-1/2} \quad (6)$$

where μ_r and ρ_r are the permeability and resistivity of the rotor, and $\nu \equiv d\mu/dH$ is between 10 and 100 times μ_r^2/B_s for most materials, B_s being the saturation magnetization. Equation (6) is valid at low ω, but falls off at high ω, especially above 10^6, because domain walls cannot respond so quickly to changes in magnetic field.

The other sources of noise depend on the time τ over which the measurement is taken, being greater for shorter τ. The maximum possible τ is the response time needed to stabilize the rotor, and is generally some fraction of the rotation period, say 1 msec for a 10,000 rpm rotor. Depending on the method used for taking the measurements, τ may be much shorter than this, increasing the noise level. This is especially important for quantum and finite electron charge noise, where there are long term correlations. With thermal and Barkhausen noise, there are no long term correlations, and taking one measurement over a long time is equivalent to averaging many measurements of shorter duration with the same total time.

In estimating the magnitude of different sources of noise, it will be convenient to use approximate expressions for the resistance, inductance and capacitance of the sensors. For inductive and eddy current sensors, it will be advantageous to make the resistance of the coil as low as possible for a given d, and this means that the length, outer radius, and thickness should all be of order d. Then

$$R_{coil} \simeq N^2 \rho_c/d \quad (7)$$

$$L \simeq N^2 \mu_0 d \quad (8)$$

where N is the number of turns, ρ_c is the coil resistivity, and μ_0 is the permeability of free space. Equation (7) is valid if the wire thickness $w \simeq d/N^{1/2}$ is less than the skin depth $\delta_c = (\rho_c/\mu_0\omega)^{1/2}$, i.e. if $\omega < NR_{coil}/L$, otherwise the resistance is increased by a factor of about w/δ_c. The capacitance of a capacitive sensor is

$$C \simeq \epsilon_0 A/d \quad (9)$$

where $\epsilon_0 = 8.85 \times 10^{-12}$ farads per meter is the permittivity of free space, and A is the area of the capacitor plates. The lead resistance is

$$R_{wire} \simeq \rho_w l_w/A_w \quad (10)$$

where the wire length l_w must be much greater than $A^{1/2}$, the cross-sectional area of the wire A_w must be less than A, and ρ_w is the wire resistivity. There is also a practical upper limit on $A^{1/2}/d$. Two other useful quantities are the maximum current density J_{max}, above which a coil or lead wire will melt, and E_{max}, the electric field at which breakdown will occur in a capacitive sensor. For copper at room temperature

$$J_{max} \simeq 4 \times 10^6 \text{ A/m}^2 \quad (11)$$

and a typical value for breakdown is

$$E_{max} \simeq 10^7 \text{ volts per meter} \quad (12)$$

For any reasonable values of the parameters, inductive and eddy current sensors are limited by J_{max},

$$I < J_{max} d^2 \quad (13)$$

and capacitive sensors are limited by E_{max}

$$I < E_{max} \omega \epsilon_0 A \quad (14)$$

although capacitive sensors could be limited by current density in the lead wires, if their cross-sectional area A_w is much less than A.

At frequencies well below kT/h, which is in the infrared at room temperature, and well below the collision frequency of electrons in the sensor, which is also in the infrared for copper, thermal noise in the voltage of a circuit has a flat frequency spectrum[8]

$$S(\omega) = kTR \quad (15)$$

where k is Boltzmann's constant, T is the temperature, R is the resistance of the circuit, and $S(\omega)d\omega$ is the average square of the voltage between ω and $\omega + d\omega$. If we wish to measure a signal at frequency ω, and take a time τ to make the measurement, then only the noise between $\omega - \tau$ and $\omega + \tau$ will interfere with the measurement, and the smallest signal (or change in signal) that can be detected will be

$$\Delta V_{thermal} \simeq (kTR/\tau)^{1/2} \quad (16)$$

Barkhausen events in a ferromagnetic material are sudden changes in magnetization that occur in a small volume v_B as H is changed, due to the sudden freeing of a domain boundary from a pinning site. "Sudden" means in about a microsecond; Barkhausen events do not occur at frequencies greater than about 10^6 Hz. They cause noise in an inductive sensor because they occur randomly, not repeating their pattern from cycle to cycle. The change in voltage in the coil associated with a single Barkhausen event in the rotor is

$$V_B \simeq \nu \omega I_c^2 N^2 (v_0/d_3)(\mu_0/\mu_r)^3(1 + \mu_r \omega d^2/\rho_r) \quad (17)$$

In deriving Eq. (17), we assumed that $(\mu_0/\mu_r)(1+d^2/\delta_r^2)^{1/2} \ll 1$, which is always satisfied for $\omega < 10^6$ Hz and $d < 1$ cm. (A safe assumption, since for $\omega > 10^6$ Hz, Barkhausen events do not take place at all.) The parameter ν appearing in Eq. (17) is defined after Eq. (6), and v_0 is the average volume over which the magnetization reverses direction in a Barkhausen event occurring at the steepest part of the B-H curve. (At lower H, the volume is proportional to H^2.) Bozorth[9] quotes average values of 10^{-15} m^3 for iron, 5×10^{-14} m^3 for 50 Permalloy, and a maximum value of 4×10^{-12} m^3, corresponding perhaps to an average value of 10^{-12} m^3, for silicon steel. The situation is somewhat complicated by the fact that if H is changed very slowly, one Barkhausen event can give rise to another, eventually resulting in a cascade of thousands of individual events, which cause a change in voltage thousands

of times greater than indicated by Eq. (17). However, this process seems to require on the order of a millisecond for each event induced, so at frequencies greater than about 10^3 Hz there should be no clustering of Barkhausen events, and Eq. (17) should be correct. If, as seems reasonable, Barkhausen events are correlated within a cycle, but uncorrelated (or substantially uncorrelated) one cycle to the next, then after averaging over a time τ several cycles long, the uncertainty in voltage due to Barkhausen events will be

$$\Delta V_{Bark} \simeq (\omega\tau)^{-1/2} V_B \qquad (18)$$

According to Heisenberg's uncertainty principle, the uncertainty in the energy in a measurement done over a time τ must be greater than h/τ, where $h = 6.6 \times 10^{-34}$ joule-sec is Planck's constant. The quantum mechanical uncertainty in a measurement of voltage, which is energy per charge, would therefore be

$$\Delta V_{QM} = h/e\tau \qquad (19)$$

This is the voltage associated with changing the magnetic flux by one quantum of flux, h/e, during a time τ; another way of stating this is that it is impossible to measure changes in flux of less than h/e, one flux quantum. Naively one might think that the uncertainty would be

$$\Delta V_{QM} \simeq h\omega/\pi e \qquad (20)$$

which corresponds to a change in flux of one quantum in half a wave period, and that averaging over a time τ much longer than a wave period would result in an uncertainty of

$$\Delta V_{QM} \simeq h\omega^{3/2}\tau^{1/2}/\pi^{3/2}e \qquad (21)$$

If the AC potential were determined by making independent measurements of the DC potential at each half wave period, and then averaging them, then the quantum uncertainty would indeed be given by Eq. (21). However, in principle it ought to be possible to make a single measurement of AC potential over many wave periods, in which case Eq. (19) would apply.

The finite electron charge $e = 1.6 \times 10^{-19}$ coulombs means that changes of current smaller than e/τ cannot be measured in a time τ. The uncertainty in voltage associated with this is

$$\Delta V_{elec}/V = e/\tau I \qquad (22)$$

This expression ought to be appropriate even for τ much longer than a wave period, since electrons are conserved, and if the current is a lower than it should be, say, during one half of a cycle, because of finite electron charge, then it ought to compensate for this in the next half cycle; the total uncertainty in charge after any number of cycles should not be greater than e.

Applying Eqs. (5), (16), (18), (19), and (22) to a typical room temperature copper inductive sensor with d = 1 cm, τ = 1 msec, $\omega = 10^4$ sec^{-1}, V = 1 volt, N = 2000, and a ferromagnetic rotor with $\rho_E = 5 \times 10^{-7}$ ohm-meters, $\mu_r = 1000\mu_0$, $v_0 = 10^{-14}$ m^3, $v = 10\mu_r^2/B_s$, B_s = 1 tesla, and $\Delta V_{digit}/V = 1.5 \times 10^{-5}$, we find

$$\delta_r \simeq 0.2 \text{ mm} \ll d, \quad \delta_c \simeq 1.2 \text{ mm} > d/N^{1/2},$$
$$R_{coil} \simeq 6\Omega, \quad R_{hys} = 6 \times 10^{-15}\Omega, \quad R_{eddy} \simeq 400\Omega,$$
$$\Delta V_{digit} \simeq 1.5 \times 10^{-5} \text{ volts},$$
$$\Delta V_{thermal} \simeq 1.5 \times 10^{-7} \text{ volts},$$
$$\Delta V_{Bark} \simeq 5 \times 10^{-15} \text{ volts},$$
$$\Delta V_{QM} \simeq 4 \times 10^{-12} \text{ volts},$$
$$\Delta V_{elec} \simeq 8 \times 10^{-14} \text{ volts}$$

The only thing that comes close to the digital noise is the thermal noise, and that could be reduced, relative to the digital noise, by increasing the voltage or decreasing the number of turns. Eventually the current density limit J_{max} would be reached, at which point

$$\Delta V_{thermal}/V \simeq (kT\rho_c)^{1/2}\tau^{-1/2}\mu_0^{-1}d^{-7/2}J_{max}^{-1}\omega^{-1} \simeq 5 \times 10^{-11} \qquad (33)$$

At this current density $\Delta V_{Bark}/V$ would increase to 1.5×10^{-11}, almost up to $\Delta V_{thermal}/V$, but far less than $\Delta V_{digit}/V$. $\Delta V_{thermal}$ could be reduced further by increasing ω, but then ΔV_{Bark} would become greater than $\Delta V_{thermal}$. The result would be essentially the same (but without Barkhausen noise) for an eddy current sensor, assuming the same parameters but with $\mu_r = \mu_0$.

We conclude that for inductive and eddy current sensors with d ≃ 1 cm, digital noise is the limiting factor, with no other source of noise coming close if the sensor is properly designed, that is if it has high enough current density and frequency (high enough flux). If it is designed with too low a flux, thermal noise could become a limited factor.

The thermal noise at the current density limit scales like $d^{-7/2}$, so if d were an order of magnitude or two smaller, as it might be in some highly miniaturized future application, thermal noise will be the limiting factor even at the current limit.

Quantum noise is negligible for inductive and eddy current sensors, if we assume that a measurement can be made over a full millisecond without "collapsing the wave function", so to speak. If the method of measurement in fact takes much less than a millisecond, even if many measurements are averaged over a millisecond, then quantum noise would be much greater, and could be the limiting factor. In particular quantum noise could exceed thermal noise if τ were small noise, since quantum noise scales like τ^{-1} while thermal noise scales like $\tau^{-1/2}$. This can happen more easily in cryogenic situations, where thermal noise will be lower, both because kT is lower and because J_{max} could be greater.

For a capacitive sensor with d = 1 mm, A = 1 cm^2, V = 1000 volts, R_{wire} = 1 mΩ, $\omega = 10^6$ sec^{-1}, τ = 1 msec, we find

$$C = 1 \text{ pf}, \quad I = 1 \text{ mA},$$
$$\Delta V_{digit} \simeq 15 \text{ mV or } 1 \text{ mV},$$
$$\Delta V_{thermal} \simeq 6 \times 10^{-11} \text{ volts},$$
$$\Delta V_{QM} \simeq 4 \times 10^{-12} \text{ volts},$$
$$\Delta V_{elec} \simeq 1.6 \times 10^{-13} \text{ volts}$$

All sources of noise other than digital noise are negligible in this case, and will be negligible for a capacitive sensor with parameters anywhere near these ones. In possible future applications with extremely small d, for example in nanotechnology, and with voltage limited by breakdown, ΔV_{elec} will eventually dominate; this would happen sooner if τ were very small.

5. Conclusions

SatCon believes that magnetic bearings and suspensions have tremendous potential for the development of extreme precision positioning systems. We believe that this technology will have a tremendous impact over the next decade in the development of a new generation of machinery for industrial and scientific applications in both terrestrial and space environment. The factors that determine achievable resolution for a magnetically suspended system are position measurement accuracy, controller bandwidth, controller gain internal noise, and external disturbance forces. Laser interferometers are expected to be available in the near future with resolutions exceeding one Angstrom and adequate accuracy for a one Angstrom resolution suspension application. Capacitive and eddy current sensors can approach these resolutions with reduced volume and cost. Based on these considerations, the authors believe that a magnetically suspended systems having resolutions in the one to 100 Angstrom can be developed using state-of-the-art and near-state-of-the-art technology.

6. Bibliography

1. Binnig, G. and H. Rohrer: Scanning Electron Microscopy. Helvitica Physica Acta, Vol. 55, pp.726-735(1982).
2. Lindsey, K. and P. Steuart: NPL Nanosurf 2: A Sub-nanometer Accuracy Stylus-based Surface Texture and Profile Measuring System with a Wide Range and Low Environmental Susceptibility. 4th Int. Precision Engr. Sem. Cransfield Inst. of Tech., U.K., p.15(11-14 May 1987).
3. Donaldson, R. and S. Patterson: Design and Construction of a Large Vertical-Axis Diamond Turning Machine. SPIE's 27th Annual International Technical Symposium and Instrument Display (21-26 August 1983).
4. Moore, W.: Foundations of Mechanical Accuracy. The Moore Special Tool Company. Bridgeport, Connecticut, pp.24-28(1970).
5. Biesterbos, J., et al: A Submicron I-Line Wafer Stepper. Solid State Technology, pp.73-76(1987).
6. Nuhn, M.; Yao, S.; Avrit, B.: I-Line Wafer Stepper Used for Low Volume Production of 0.5 Micrometer GaAs Integrated Circuits. Solid State Technology, pp.81-84(1987).
7. Berthold, J.; Jacobs, S.; Norton, M.: Dimensional Stability of Fused Silica, Invar, and Several Ultra-low Thermal Expansion Materials. Metrologia 13, pp.9-16(1977).
8. Reif, F.: Fundamentals of Statistical and Thermal Physics. McGraw-Hill, pp.587-594(1965).
9. Bozorth, Richard M.: Ferromagnetism. Van Nostrand, New York. pp.524-532(1951).